

## **Effect of color on scratch and mar visibility of polymers**

L. De Noni<sup>1,2</sup>, S. M. H. Marjuban<sup>1</sup>, L. Andena<sup>2</sup>, , K. Noh<sup>1</sup>, Y. Li<sup>3</sup>, P. Vollenberg<sup>3</sup> and H.-J. Sue<sup>1,\*</sup>

<sup>1</sup>Polymer Technology Center, Department of Materials Science Engineering, Texas A&M University, College Station, TX 77843-3123, US

<sup>2</sup>Dipartimento di Chimica, materiali e ingegneria chimica "G. Natta", Politecnico di Milano, Milan, Italy

<sup>3</sup>SABIC's Specialties business, Mount Vernon, IN, US

\* Corresponding author:

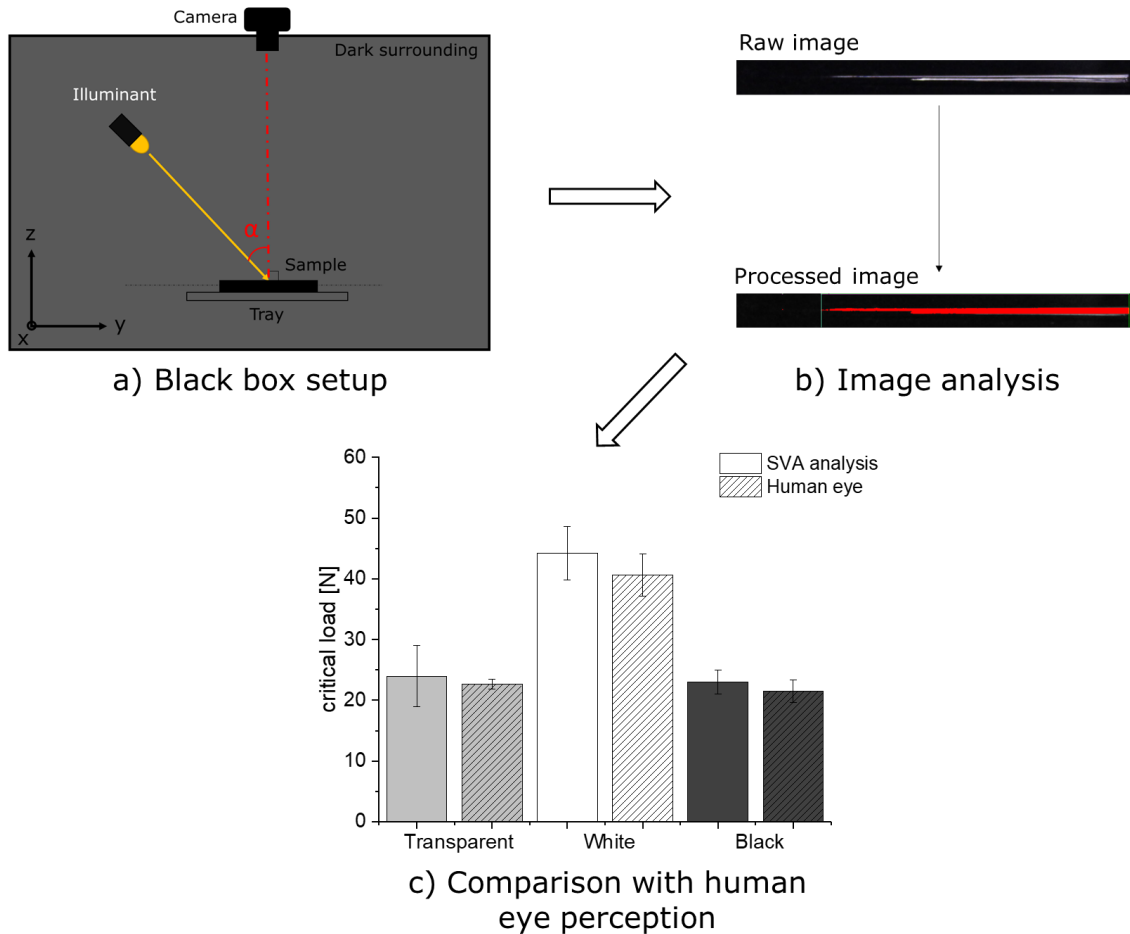
Hung-Jue Sue

Polymer Technology Center, Department of Materials Science Engineering  
Texas A&M University, 575 Ross Street  
College Station, TX 77843-3123, US

E-mail: [hjsue@tamu.edu](mailto:hjsue@tamu.edu)

### Graphical abstract

Scratch and mar visibility is measured through a purposely designed black box. The present method for the quantification of the scratch visibility agrees with human eye evaluation. The color of the material has a crucial effect on the scratch visibility. Experimental procedure to measure the scratch visibility is shown in the graphical abstract: a) the scratched sample is located into the black box setup; b) the images taken in the step "a" are analyzed to quantify the onset of visibility; c) the results are quantitatively compared to the human eye perception of the scratch.



## Abstract

Scratch and marring phenomena can affect the perceived quality of many products. This work relates to methods to quantitatively evaluate the effect of sample color on polymer scratch and mar induced visibility, in view of linking scratch behavior with the underlying physics. A custom-built black box was utilized for the analysis of the samples with different colors and surface finishing. A white color was shown to delay the onset of visibility by reducing the contrast between the damaged and undamaged area, which is in good agreement with the human eye perception. The same results were found for the mar phenomenon, highlighting how the white color is able to mask the damage. The usefulness of the present work is discussed and some perspectives for the future work are presented.

**Keywords:** Scratch, mar, color, polycarbonate, visibility.

## Introduction

Polymer scratch and mar behavior has been widely studied in the last three decades. There are several areas of concern regarding scratch, namely aesthetics, structural integrity, functionality and durability. The aesthetics is a key requirement for most commercial products. Visible scratches, marring or any surface defects reduce the perceived quality of polymeric products. Despite several publications describing the relationship between polymer mechanical properties and scratch deformation [1-5], their impact on scratch visibility is still not well understood. Scratch deformation mechanisms are strictly related to environmental conditions (e.g., temperature, humidity, ageing) [2, 6-8], presence of particles/third bodies, scratching conditions (sliding velocity, contact pressure, indenter geometry, etc...) [9-11] and material properties, such as modulus [1], yielding [5], strain hardening [12, 13] and so on. Finite element method (FEM) analysis has been shown to be a useful tool to describe and partially predict the scratch behavior of polymeric materials [13-16]. In any case, additional research is necessary to improve the current models for predicting accurately the scratch deformation mechanism and damage profile.

The presence of surface defects and deformation, such as scratch and mar, may modify the polymer surface appearance and color [17]. At the same time, physical damage can also alter the phenomena involved in light interaction with material surfaces, such as light scattering and refraction [18], which in turn influence the related aesthetical properties as perceived by the human eye. Some studies attempted to quantitatively measure the scratch visibility [18-29]. However, uncertainty emerges on an apparent effect of sample gloss and color on scratch visibility. For instance, one may claim that the detection of the scratch-induced stress whitening phenomenon onto a white background becomes more difficult with respect to black surfaces. All these factors, namely scratch deformation mechanism, gloss, and color, contribute to the scratch visibility phenomenon. The understanding of the possible effect of gloss and color on scratch visibility is crucial for gaining fundamental knowledge of polymer scratch resistance. Unfortunately, no systematic study can be found on how and why the sample color influences scratch and mar visibility. What is lacking so far is the understanding of the possible physical phenomena involved in the visibility, a way to quantify such phenomena with some representative parameters, and the understanding of how this relates and matches with the human eye perception. Also, it would be useful to develop proper models in order to predict the scratch and mar visibility.

The human eye can perceive colors depending on the wavelengths of the light impinging the retina, on luminance, the contrast, and also on material roughness. All these factors (some related to the surface, some to the lighting conditions) may depend on the peculiarities of the individual human eye, such as visual acuity, pupil size, retinal eccentricity and age [30]. In particular, the human eye can capture the contrast between an object and its background, allowing us to discriminate and differentiate objects. Contrast, defined as the ratio of the difference in luminance between an object and the background over the overall luminance [31, 32], is a parameter relevant to the visual perception of scratches [18, 23]. Developing a method which can reproduce these aspects is crucial for the purpose of flaw detection. Contrast can be given by differences in luminance, which involves both “achromatic” and “chromatic” contrast [33]. An object can be identified when the relative contrast against the background is greater than the minimum threshold detectable by the human eye. It has been shown that humans are able to detect contrast variations as small as 0.5% [34-37]. However, the minimum detectable contrast is typically higher in most cases (around 2%). It is worth noting that this contrast sensitivity is dependent on several factors, namely luminance, viewing angle and individual human eye property, i.e., quality of the eye lens, the sensitivity of photoreceptors and some intrinsic morphological characteristics [38]; a detailed review can be found elsewhere [39]. If the shape of an object is defined, contrast for identification can be used to determine the phenomenon, specifically the detection of surface defects such as scratch and mar.

Among the many material properties that can affect the scratch visibility, the focus of the present research is to highlight the effect of color. The aim is to investigate whether color can affect scratch and mar visibility and to obtain insight on the underlying physical phenomena. The human visual system comprises an abundance of physiological and psychological intricacies related to not easily accessible physical properties; therefore, most available experimental techniques lack do not provide an effective characterization. In this sense, if any effect is observed, the aim should be to quantify such phenomenon with a representative parameter. To do so, the effect of color and deformed surface profile on the scratch visibility must be separated. Also, these findings must be related to the perception of the human eye. Despite the different deformation mechanisms involved in scratch and mar damages, the goal of this work is to try to measure the visual effects of color on both phenomena.

## Experimental section

### 2.1 Materials

Both glossy and matte surfaces were considered in the present work. Injection molded glossy samples made of BPA-homo-polycarbonate and a polycarbonate copolymer were produced with dimensions of 100.0 mm x 100.0 mm x 3.2 mm and provided by SABIC's specialties business. Both polycarbonate (PC) and polycarbonate copolymer (COP) samples came with transparent, black and white colors. The former have been labelled as PC-N (transparent), PC-B (black) and PC-W (white); the latter were named COP-N (transparent), COP-B (black), and COP-W (white). Black samples contain (among other fillers) carbon black, whereas titanium dioxide (TiO<sub>2</sub>) pigment was used for the white ones.

Matte samples were obtained by spraying polyurethane coating (AkzoNobel, Sprint Coating Finish B/691) onto an injection molded black glossy polycarbonate (Makrolon® AX2677) substrate. Substrates were produced with dimensions of 50 mm x 50 mm x 3 mm. Coatings with four different colors (white, grey, green and red), were manually deposited onto the surface of the substrate. The thickness of the coatings was around 35 ± 5 µm.

### 2.2 Scratch and mar test

Scratch tests were performed using a spherical indenter made of stainless steel, having a diameter of 1 mm. For glossy samples, a normal load linearly increasing from 1 to 130 N was applied at a constant sliding velocity of 100 mm/s, over a scratch length of 80 mm. Different scratch test parameters were selected for matte samples, due to the shorter sample dimensions (50 mm x 50 mm): in this case the normal load varied from 1 to 50 N, over a scratch length of 35 mm, sliding over the surface at a constant speed of 1 mm/s. The tangential and normal forces were recorded during the scratch test. The scratch apparent coefficient of friction (SCOF), defined as per equation 1, was measured in both cases to investigate the scratch behavior of the selected materials. Eight scratches were performed on each material (on 2 different specimens) and highly reproducible results were obtained (within 10% in terms of tangential force  $F_t$ ); therefore, average curves only will be shown in the results section. Compressed air was used to remove any possible contaminants from both tip and samples surface.

$$SCOF = \frac{F_t}{F_n} \quad (\text{Eq. 1})$$

The mar test was performed by utilizing a self-aligned stainless-steel tip to generate the mar damage on the sample surface. The tip has a flat square surface with an area of 7 mm × 7 mm; a 4000-grit sandpaper was attached onto the mar tip using a double-sided tape (Scotch® Indoor Mounting Tape), as shown in Figure

1. The test was performed by applying an increasing linear load from 1 N to 8 N, over a scratch length of 70 mm at a constant sliding speed of 10 mm/s. The test parameters were chosen in accordance with common automotive standards. Only glossy samples were analyzed. Five mar tests were carried out on each sample. New sandpaper was utilized for each mar test. All the scratch and mar tests were performed along the injection flow direction.

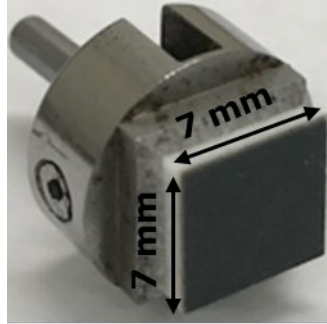


Figure 1. Self-aligning tip employed for the mar tests: the 4000- grit sandpaper was stuck onto the tip surface through a double-sided tape. The sandpaper area is 7 mm x 7 mm.

### 2.3 Confocal laser microscope

A high-resolution Keyence VK9700 violet laser scanning confocal microscope (VLSCM) was used to analyze the scratch deformation and evaluate the average surface roughness ( $R_a$ ) of the materials under investigation (reported in Table 1), as defined in equation 2:

$$R_a = \frac{1}{l} \int_0^l |z(x)| dx \quad (\text{Eq. 2})$$

where “ $l$ ” is the sampling length. The value is averaged over an area of  $1350 \mu\text{m} \times 1012 \mu\text{m}$ .  $R_a$  was measured by analyzing 5 different regions and the average value is reported in Table 1. Glossy samples (PC and PC copolymer) had a comparable surface  $R_a$ . The same holds for the matte samples, although with a significantly higher value compared with PC/COP ones. The machine was also used to analyze the relevant scratch deformation mechanisms and to quantitatively measure the scratch profile at specific values of the applied normal load.

Table 1. Average roughness ( $R_a$ ) value for glossy (top) and matte samples (bottom).

	PC-N	PC-W	PC-B	COP-N	COP-W	COP-B	PU white	PU grey	PU red	PU green
$R_a$ [ $\mu\text{m}$ ]	$0.08 \pm 0.01$	$0.11 \pm 0.02$	$0.08 \pm 0.01$	$0.08 \pm 0.01$	$0.11 \pm 0.01$	$0.11 \pm 0.02$	$1.07 \pm 0.04$	$1.25 \pm 0.09$	$1.27 \pm 0.11$	$1.33 \pm 0.09$

The VLSCM was also employed for measuring the topographical information of the marred regions. The average roughness  $R_a$  was measured at different locations (normal loads) along the mar regions. The data reported are the average of 5 measurements (one per each mar region) taken at about 3, 5 and 7 N.

## 2.4 Gloss measurements

Gloss measurements were performed using a BYK-Gardner micro-TRI glossmeter. The data were taken at 20° and 85° for glossy and matte samples, respectively, according to the ISO 2813 standard [40]. The results, expressed in Gloss Units (GU), are briefly shown in the Table 2. Transparent samples were placed on a light absorbing black cloth background. No significant differences were reported within results obtained on glossy samples. The same can be stated for the matte coatings.

Table 2. Gloss values expressed in gloss units (GU) for glossy (top) and matte (bottom) samples taken at 20° and 85°, respectively.

	PC-N [20°]	PC-W [20°]	PC-B [20°]	COP- N [20°]	COP- W [20°]	COP- B [20°]	PU white [85°]	PU grey [85°]	PU red [85°]	PU green [85°]
<b>Gloss units [GU]</b>	180.0 ± 1.9	113.3 ± 0.5	113.4 ± 0.5	177.0 ± 2.5	113.6 ± 0.7	113.7 ± 0.5	10.9 ± 0.3	9.4 ± 0.2	10.0 ± 0.1	8.8 ± 0.1

Gloss measurements were also performed for the determination of the effect of the mar damage on the specular reflection of the light. The average gloss value was measured at different locations (and correspondingly normal loads) along the mar regions. Each reported value is the average of 5 measurements (one per each mar region) taken at about 3, 5 or 7 N.

## 2.5 Scratch and mar visibility analysis

### 2.5.1 Scratch visibility analysis

The images of scratched regions were captured by utilizing a high-resolution camera (Canon EOS REBEL T3i DSLR with Canon EF-S 18–55 mm zoom lens) inside a black box setup based on fluorescent bar-shaped CIE D65 light source (Figure 2a). Walls of the custom-built black box setup (690 mm x 430 mm x 690 mm) were covered with absorbent black cloth to suppress light reflection. The samples were located at the middle of the tray (Figure 2a). A black cloth was used as a background for the transparent samples. The camera was set at ISO-800 and the exposure time at 1/30 s. The angle  $\alpha$  (Figure 2a) between the camera and the illuminant was set at 30° or at 75°. At 30°, the light interaction with the scratch results in a brightened area for all the tested samples. At 75°, instead, this interaction turns into both darkened and brightened areas. The camera was always aligned perpendicular to the scratched surface. Moreover, the projection of the incident light direction on the surface was perpendicular to the scratching direction, as shown in Figure 2b [18]. The images were subsequently analyzed with the Automatic Scratch Visualization (SVA) software donated by Surface Machine Systems (Austin, Texas). The parameter considered by the software is the *contrast* between scratched area and undamaged regions (background). In particular, the contrast is defined according to Equation 3 [31, 32]:

$$C [\%] = \frac{I_s - I_b}{I_s + I_b} * 100 \quad (\text{Eq. 3})$$

where  $I_s$  is the luminance of the scratched area and  $I_b$  is the luminance of the background. A preliminary analysis of the effect of the camera settings was carried out with an aim to find the proper conditions to reproduce the human eye perception. The image analysis was performed by varying the contrast values

from 3.0% to 1.0% to match human eye assessment results. The SVA software evaluates the contrast by comparing each pixel line of the damaged area compared to background area nearby, as shown in Figure 3a. The scope of the analysis is to study a range of different scenarios to understand how lighting conditions affect the onset of scratch visibility and to compare the behaviors among the samples of different colors. Visibility can be induced by both brightening and darkening phenomena depending on the relative orientation of illuminant and scratch. Either case was considered to determine the worst-case scenario. There are several reasons for doing so. Firstly, the analysis of defects typically happens under different scenarios and a single observation angle would not be enough to describe the overall behavior of the colored materials. Secondly, different colors might behave differently at different angles. The aim is to identify the worst-case scenario for each color and then compare the relative performances. Both brightening and darkening phenomena were considered for the determination of the worst-case scenario. However, only brightening, determined to be the worst-case scenario, was further analyzed to determine structure-property relationship.

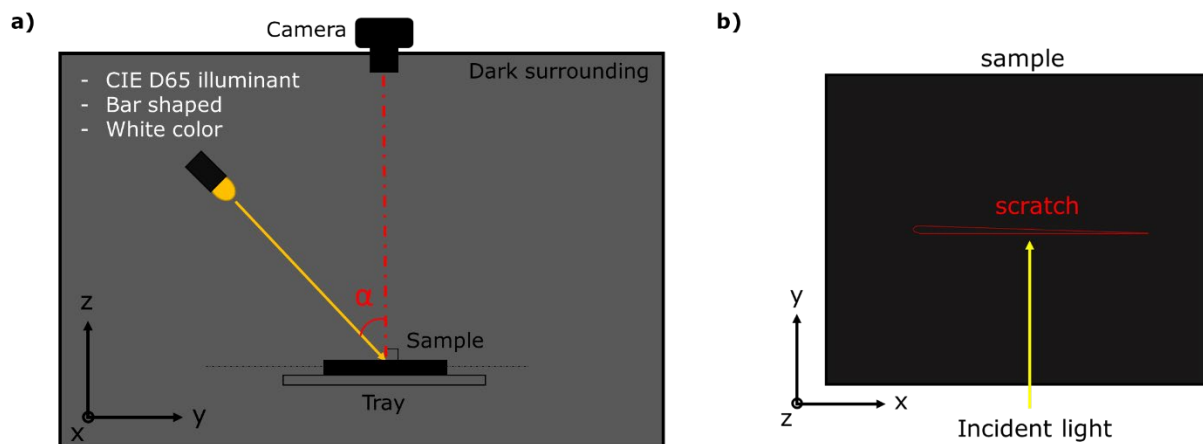


Figure 2. a) Sketch representing the custom-built black box setup. The sample is placed onto the tray and the illuminant can be rotated at a certain angle  $\alpha$  (at a fixed distance from the samples). The camera is aligned with the normal to the surface of the samples. b) The projection of the incident light direction is perpendicular to the scratching direction.

### 2.5.2 Mar visibility analysis

The same procedure was carried out for mar analysis. The images were taken at  $35^\circ$  employing the same camera settings. The chosen angle in this case does not lead to significant differences in the outcome, and its value was selected with no particular relation to that employed during scratch testing. The image analysis procedure works in the same way as previously described, this time considering the full width of the marred area (7 mm, as shown in Figure 3b).

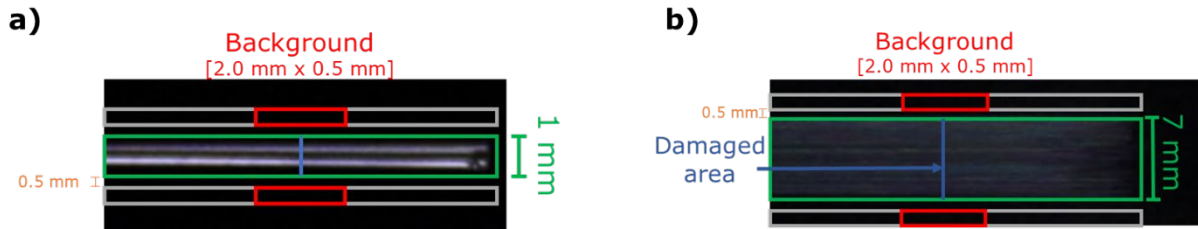


Figure 3. Schematic representation showing how the SVA software analyzes the (a) scratch visibility and (b) mar visibility.

## 2.6 Human eye assessment (Psychophysical test)

The human eye assessment was performed by at least 8 trained surveyors to detect the onset of visibility for at least 5 scratches per sample. They were taught how to determine the onset of visibility. To do so, the black box setup was used as shown in Figure 4. The room was darkened while performing the assessment. Five surveyors were also asked to rank the mar damage according to its severity for all the glossy tested samples utilizing the same setup at 35° (Figure 4).

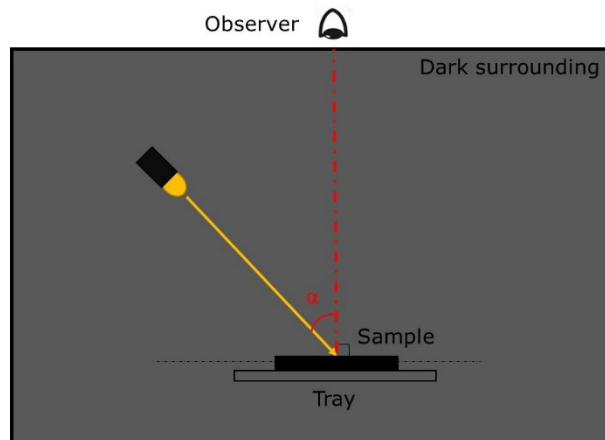


Figure 4. Sketch representing the experimental setup for the human eye assessment.

## 3. Results and discussions

Results were grouped into two separate sections since glossy and matte samples experience different deformation mechanisms. Also, mar analysis was kept separated because of the different physics behind the mar process.

### 3.1 Scratch of glossy materials

#### 3.1.1 Scratch visibility

Human eye assessment and SVA software analysis were performed with the aim of identifying the onset of visibility. The onset of visibility is defined in terms of the critical load at which the scratch becomes visible. Visibility depends on the lighting conditions and the relative orientation of the scratch with respect to the illuminant [18]. At 30° vertical illuminating angle, results of the human eye assessment are compared to



SVA software analysis in Figure 5. The contrast value for the analysis is set at 1.0% for all the samples as it matches the human eye assessment data well. This shows that the setup presented in this study can reproduce human eye perception. Also, it is shown that contrast can be selected as a representative parameter for describing scratch visibility, which means that the contrast is playing a crucial role in the visibility regardless of the color of the sample. The white color shows higher critical load values. This could be related either to the scratch deformation mechanism or to the color itself. Since the lighting conditions significantly affect the critical loads at which visibility occurs, the analysis was also carried out at  $75^\circ$  as another extreme scenario for showing the darkening effect. Figure 6 shows the results of the human eye assessment compared to SVA software. The results highlight an opposite trend, that is, the black and transparent samples show higher critical loads for the onset of visibility. Different lighting conditions generate different scenarios. Brightening or darkening phenomena can take place, impacting the onset of scratch visibility differently according to the color of the sample. However, by comparing the data at  $30^\circ$  and  $75^\circ$  illuminating conditions, the worst-case scenario appears to happen at  $30^\circ$  for all tested samples. Therefore, this scenario is giving the worst overall performance of the selected materials, and under this condition sample colors can be compared. It also will be relevant to developing a physical model to understand and predict how the scratch profile interacts with the incident light, the angle of illumination and the observation position to predict brightening and darkening phenomena in future works. To understand the reason why white sample shows a higher scratch visibility resistance, scratch deformation mechanisms were studied and presented below.

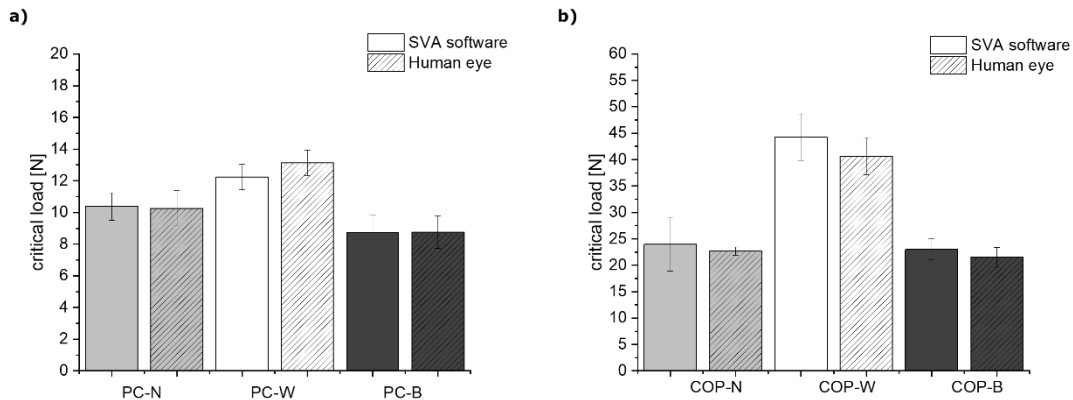


Figure 5. Results of the human eye assessment and SVA software at  $30^\circ$ : (a) PC samples and (b) PC copolymer samples.

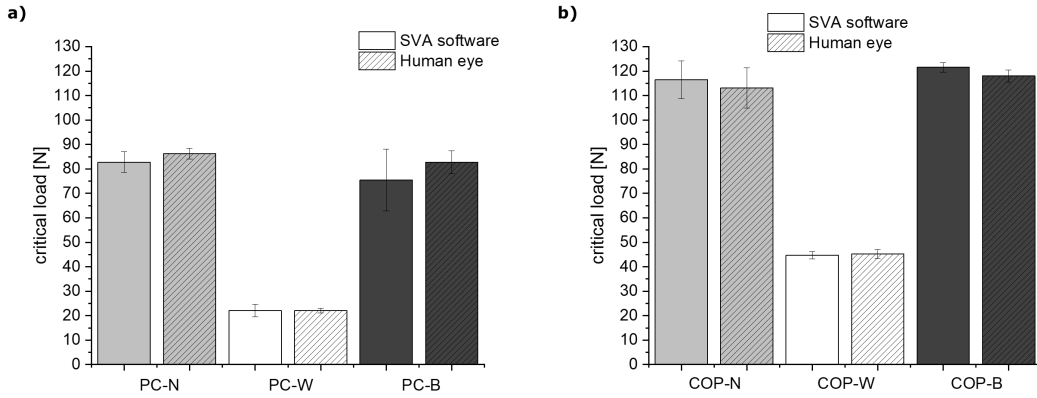


Figure 6. Results of the human eye assessment and SVA software at 75°: (a) PC samples and (b) PC copolymer samples.

### 3.1.2 Scratch behavior, deformation mechanisms and scratch geometry

The scratch coefficient of friction (SCOF) was evaluated as shown in Figure 7. It was previously demonstrated that a higher SCOF typically leads to lower scratch resistance [41, 42]. In this sense, PC samples show higher SCOF (with respect to COP ones), which should result in a lower scratch resistance. The SCOF is not affected by the color of the samples.

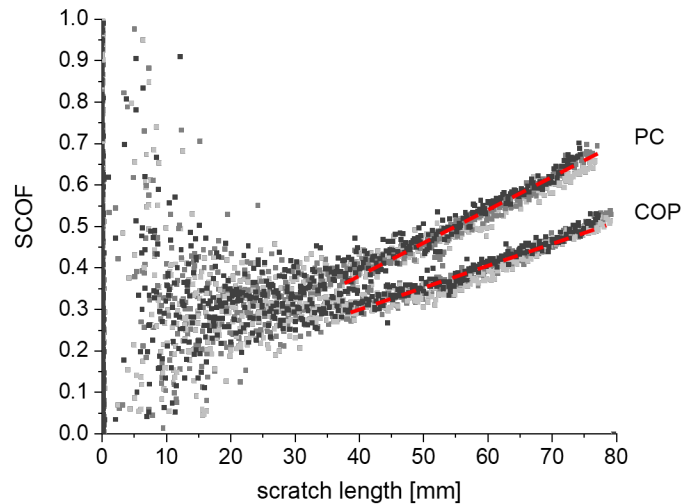


Figure 7. Scratch coefficient of friction (SCOF) curves: two different trends are highlighted for PC and COP samples.

The scratch-induced deformation profiles were investigated using VLSCM. All the tested glossy samples show the same deformation mechanism (Figure 8): materials first experience ductile ploughing which results in ductile ploughing deformation + crack formation inside the scratch groove as the normal load approaches approximately 60 N and 80 N for the PC and COP samples, respectively. At high loads (above 100 N), cracking and stress whitening are observed at the bottom of the scratch groove. Since the onset of

visibility occurs at loads lower than 60 N for all tested samples, ductile ploughing is the mechanism relevant to scratch visibility. There is no difference in the scratch deformation profile in terms of residual depth and shoulder height, irrespective of the color (Figure 9). PC samples have higher depth and larger pile-up (shoulder height) compared to COP samples at the same normal load, which also explain why they have lower critical onset load for visibility. No scratch groove was observed for COP samples around the critical load for the visibility of PC samples at around 10 N. This is in agreement with SCOF data.

It is also worth noticing that the onset of visibility appears to be located where the scratch residual depth and shoulder height are about 2.5  $\mu\text{m}$  and 2.0  $\mu\text{m}$ , respectively, for both PC and COP samples. Also, the scratch profile is not affected by neither the white pigment nor the black dye. This means that the differences in scratch resistance reported in Figures 5 and 6 must be related to the color alone. There is no relevant difference for black and transparent color for both PC and COP samples. This is explained by the fact that they have the same scratch profile, gloss and color due to the black cloth used as a background for the transparent sample in the analysis. In this way, it becomes possible to separate the contribution of the scratch deformation profile and color on scratch visibility. To understand the reason behind the above observed phenomenon, deeper insights are provided in the next section, where the role of the color on contrast has been studied.

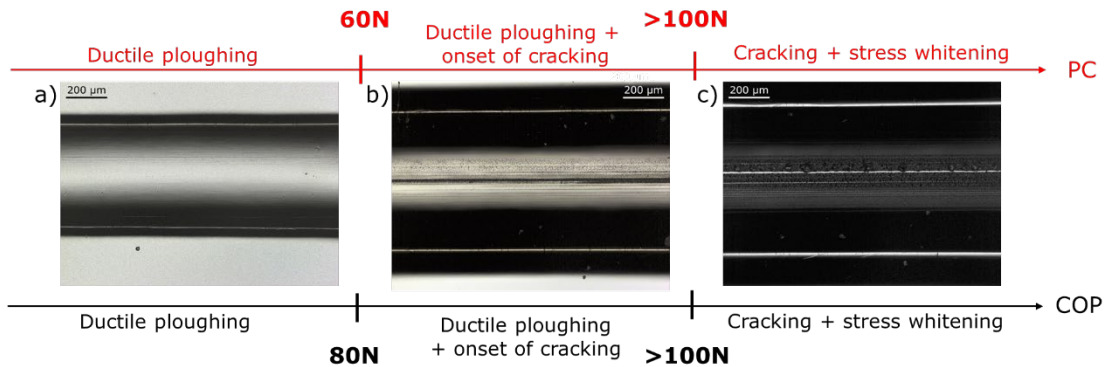


Figure 8. Summary of the scratch deformation mechanisms involved in the scratch phenomenon: a) ductile ploughing up to 60 N (PC samples) and 80 N (PC copolymer) samples, b) where onset of cracking occurs inside the scratch groove, and (c) eventually materials experience stress whitening (above 100 N). Reference images are shown for PC.

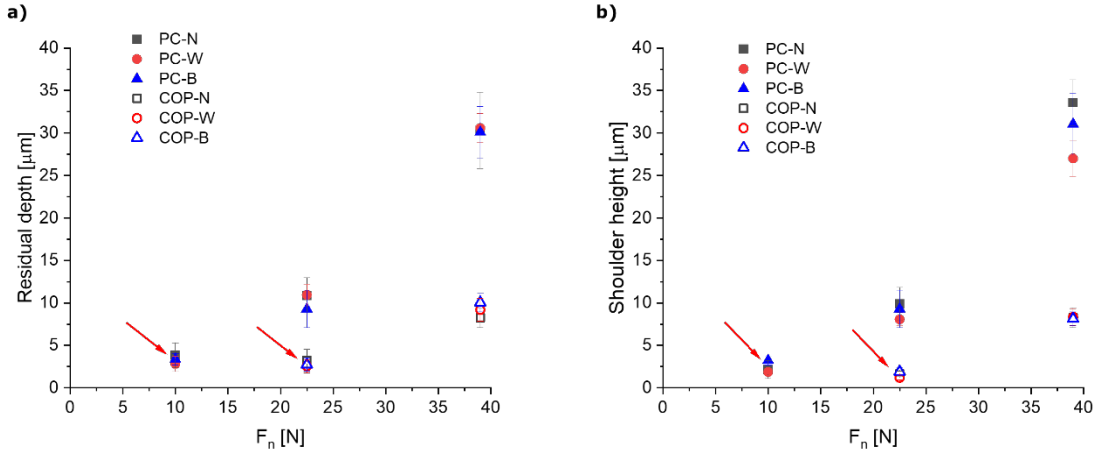


Figure 9. Scratch geometry: (a) scratch residual depth and (b) shoulder height. The red dotted lines indicate the scratch geometry at the onset of visibility.

### 3.1.3 The effect of color on contrast

Light can interact with matter in different ways. Light can be reflected at the interface between air and the sample following the Fresnel law. The light is reflected in the specular direction with respect to the normal at the surface at each location. This phenomenon is related to the angle of incidence of the light and refractive index of the material, which is in turn dependent on the light wavelength. However, the refractive index for plastic materials is only slightly dependent on the light wavelength across the visible spectrum [43-45]. In this way, the reflectance spectrum always resembles the incident light spectrum. In our case, daylight CIE D65 has been utilized, being white in color. The light can also penetrate into the material, where it can be either scattered by the colorant towards the same interface it came from or absorbed by the colorant itself. The interaction between the light and the colorants gives the material its characteristic color. The light can also be transmitted through the material. A simple mathematical model was proposed by Shafer [43], called “*dichromatic reflection model*” (Equation 4):

$$L(\lambda, i, e, g) = L_i(\lambda, i, e, g) + L_b(\lambda, i, e, g) = m_i(i, e, g) * c_i(\lambda) + m_b(i, e, g) * c_b(\lambda) \quad (\text{Eq. 4})$$

where  $\lambda$  is the light wavelength, “ $i$ ” is the angle of incidence, “ $e$ ” is the angle of the reflection and “ $g$ ” is the angle between the specular and off-specular reflection directions. The total luminance of the reflected light is given by two components: the luminance  $L_i$  of the light reflected at the interface sample-air and the radiance  $L_b$  of the light reflected by the bulk (colorants) of the samples. Each component is given by two terms, the spectral power distribution (color)  $c_i$  or  $c_b$ , and its magnitude  $m_i$  or  $m_b$ , which depends only on the geometric angles of the reflected light. The model assumes that the relative magnitude of each process is a function of the magnitude factor  $m_i$  (or  $m_b$ ), which means that the illuminating angle, the geometry of the surface and the relative viewing position determine the intensity of each process.

In our research, the presence of the scratch on the surface modifies light reflection. This results in a brightened, whitened area, which is related to the spectrum of the light reflected at the material-air interface, being white in color, where “ $L_i$ ” is the dominant component. Specifically, this phenomenon occurs with a different magnitude at each normal scratch load level because of the different geometry introduced at those specific conditions. The reflectance spectrum of the surrounding, intact area is characterized by the intrinsic material color originated by the interaction of light with the bulk of the material, where “ $L_b$ ” is the dominant

component. The result of this phenomenon is that the human eye can perceive a brightened area because of the scratch (Figure 10). Since the phenomenon is dependent on the scratch geometry, which varies with the increasing normal load, there is a specific location at which this brightened area becomes apparent, defined as the onset of visibility for the human eye.

As mentioned above, human eye can detect and differentiate objects by their color and contrast. However, the contrast between the scratched region and the intact background depends on the color of the background itself. Therefore, detection of the onset of visibility might be delayed by reducing the contrast between scratch and background below the minimum threshold of the human eye. This concept is of significance, because it implies that the background plays a crucial role in determining the onset of visibility. For instance, human eye can have difficulties in detecting object with a specific color onto a background with the same color. As a matter of fact, white color seems to delay the onset of visibility in the present study. The reason for this lies in the differences in luminance between the scratch and the background. As mentioned, the spectrum color of CIE D65 illuminant resembles the daylight being white in color, so the reflected light at the interface sample-air is characterized by the same white color. At the same time, the intact surface is still white in color because of the white pigment. The similarity of the reflectance spectra between deformed and intact area delays the onset of visibility because the human eye is not capable to perceive such small differences in luminance. Vice versa, when the background is black, the different spectral power distribution between the damaged area, which is still subjected to brightening phenomenon, and the spectral distribution of the undamaged intact surface is marked and sharp, determining a significant contrast which is easily detectable by the human eye.

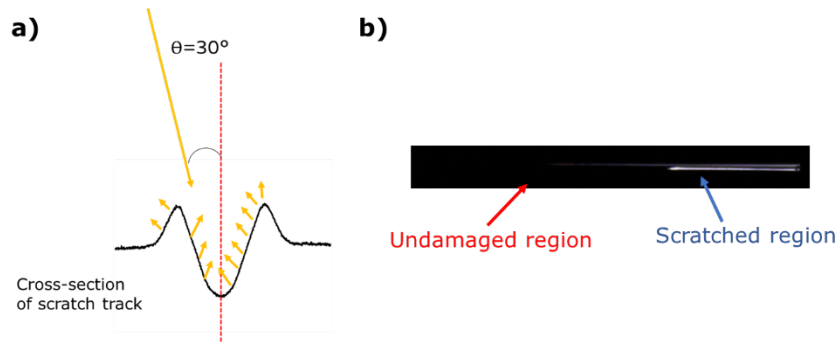


Figure 10. (a) Schematic representation of the effect of the scratch geometry on the light reflection phenomenon. (b) Image taken at  $30^\circ$  for the black PC copolymer sample showing the resulting light-sample interaction (on the right).

In fact, if the contrast is increased from 1.0% to 3.0% in 0.5% per step with the SVA software (Figure 11) for the images taken at  $30^\circ$ , black and transparent samples show almost a constant trend of the critical load and small deviations of the data for each contrast value. On the other hand, white color experiences an increase in the critical load for the onset of visibility with the selected contrast value. This shows how sensitive the detection of the visibility onset is when the background is white. The software was shown to give good agreement with the human eye perception when the value was set at 1.0%. As a matter of fact, the contrast value seems not to really matter for transparent and black samples, which means that the results are not changing at higher contrast threshold value. Therefore, the contrast is already high enough to lead to visibility. In the same way, the results show that the human eye can detect much more easily the onset

of visibility for black and transparent samples because of the high contrast. The dependence of the critical visibility load on contrast level is more pronounced for the white PC copolymer than that for the white PC because of the large deformation occurring on all the PC samples as a consequence of the scratch. It is worth noting that the differences in the local luminance between the brightened area, which is related to the scratch groove and the undamaged intact background are strictly related to the color of the background itself and can significantly modify the onset of visibility.

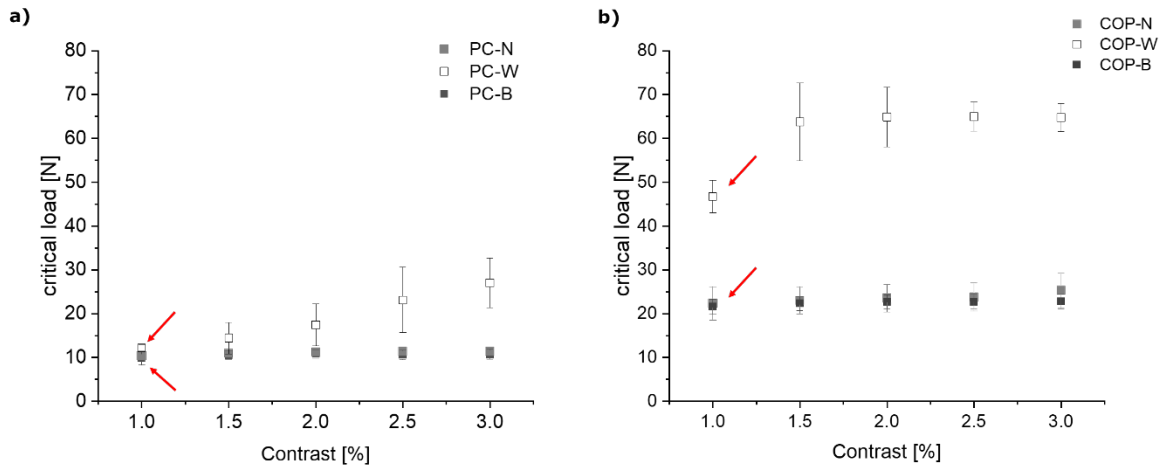


Figure 11. The graphs show the effect of different contrast parameters on the detection of the critical load for the onset of visibility for (a) PC samples and (b) PC copolymer samples at 30° viewing angle. The contrast value of 1.0% was used for the analysis shown in Figures 5 and 6. The red arrows point out the selected contrast values to match the human eye results.

### 3.2 Scratch visibility of matte samples

In the previous section, the analysis is basically restricted to glossy white and black samples. Therefore, matte coatings with different colors (white, grey, black, red and green) were considered to broaden the array of tested samples and validate the methodology proposed in the case of more limited color differences. As already mentioned, both the color and the surface gloss [23] can affect the scratch visibility. The main difference between matte and glossy surfaces is their ability to reflect the light, in particular in the specular direction. Glossy surfaces are typically characterized by lower roughness values and can reflect a greater amount of light in the specular direction compared to the matte ones. Therefore, it is worth investigating the effect of color on the scratch visibility also for the latter type of surfaces. To do so, the same testing procedure described before was followed; however, different scratch test parameters were selected because of sample dimensional constraints. Matte samples may experience different scratch deformation mechanisms, namely ironing (reduction of the surface roughness) at low loads, which precedes ductile ploughing; for comparison purposes, only brightening related to this latter deformation mechanism was considered. It is worth noting that all tested samples showed comparable scratch profiles at a given normal load. The results at 30° are condensed in Figure 12, as a function of the contrast variation considered as a threshold for scratch detection. The agreement between image analysis and human eye was good (as previously demonstrated for PC/COP) and it is not shown in the graph. White color samples again display lower scratch visibility, for the same reasons discussed previously. If we neglect the effect of the ironing phenomenon on visibility, the contrast reduction due to the white color is clearly delaying the visibility onset. All colored samples show the same trend (Figure 12). The variations of the onset of critical load with

contrast are less sensitive compared to what was shown for glossy samples, specifically for the white ones. The surface roughness reduces the amount of the specular reflected light, thus reducing the luminance of the brightened area. In turn, this leads to a reduction of the contrast between damaged and undamaged areas, which explains why the effect of contrast on the scratch visibility is flattened as the set contrast value increases. Also, it is worth noting that the green color shows higher scratch visibility. This is in good agreement with human eye perception: the critical load measured by the software shows slightly higher values, but the ranking between the colors is consistent, i.e., the critical load is higher for white samples, and lower for the green ones. This phenomenon is related to the different sensitivity of the human eye to colors under daylight conditions [18]. It is known that the human retina is more sensitive to the green color with respect to red and blue, located at the ends of the visible spectrum. These results also give insights regarding the effect of the color for matte surface with comparable surface roughness.

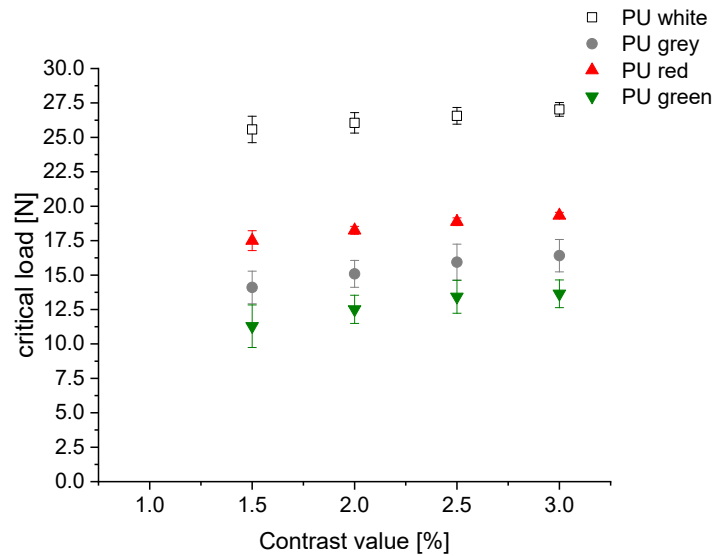


Figure 12. The effect of contrast on the onset of visibility on PU-coated PC samples in white, red, grey, and green colors.

### 3.3 Mar visibility of glossy polycarbonate and copolymer polycarbonate samples

Compared to scratch, mar damage involves different damage mechanisms, with a different physical origin [46]. The friction behavior is measured as defined in Equation 1 (mar coefficient of friction, MCOF) and shown in Figure 13. At low loads, the data are quite noisy because of inertial effects, amplified by the higher friction conditions present during mar testing. When the load increases, an almost constant trend is observed for all tested samples with no detectable differences.

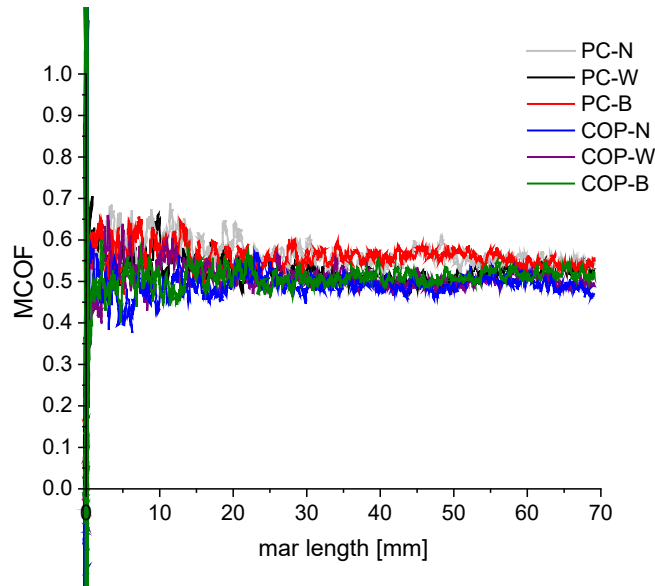


Figure 13. Mar coefficient of friction (MCOF) for PC and PC copolymer samples.

In a practical sense, mar is mostly of concern to glossy surfaces [23]. In this study, the effect of color on the mar visibility was investigated using the PC and COP samples already studied above. The aim is to quantify the mar visibility as a function of the color alone, therefore neglecting the geometric contribution (if possible). It was shown that mar visibility may be related to surface roughness changes [46]. In fact, the damaged area suffers a roughness increase due to the marring tip sliding as highlighted in Figure 14a, where the Y axis represents the difference between the roughness of the marred area and the undamaged one. An increasing trend is observed for all tested samples, which is related to the increasing contact pressure. It is evident that COP samples can resist sandpaper roughening better than PC samples. The increase in the surface roughness affects how the light is reflected on the surface; as a result, the decrease in the intensity of the specular reflected light and the increasing amount of the off-specular light scattering lead to greater mar visibility. Figure 14b shows that the specular gloss (expressed in gloss units) of the surface is decreasing with the increasing normal load, i.e. with the severity of the damage. Also, it is possible that the material is experiencing stress whitening because of localized yielding phenomena, which may in turn cause color changes that can also impact the aesthetical quality of the surface.



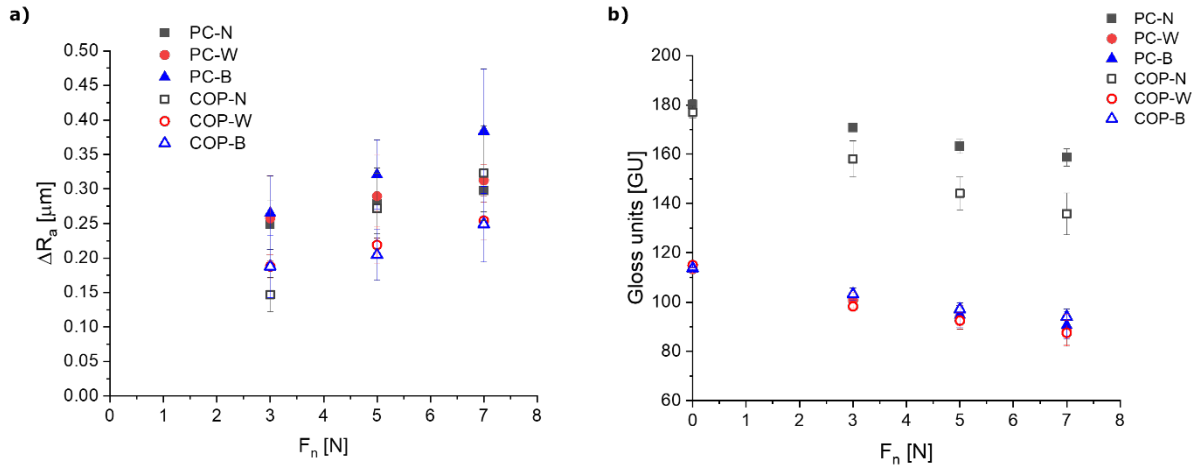


Figure 14. a) The difference of surface roughness between scratched and unscratched area ( $\Delta R_a$ ) is plotted against the increasing normal load. An increasing trend with force is observed for all tested samples. b) Variations of surface gloss as a function of the applied normal load from 0 N (undamaged) to 7 N. A decreasing trend is observed for all tested samples.

Image analysis was performed as described in the experimental section to obtain the contrast curve, reported in Figure 15a. The trend is either increasing or leveling off for all the curves, so the area under the curve was arbitrarily selected as the representative parameter and calculated as shown in the Figure 15b. It is worth noticing that this parameter is considered as a sort of index on the severity surface damage: the higher the value, the higher the contrast between damaged and undamaged surfaces and the lower the mar resistance of the material. As shown, the black and transparent PC samples display lower mar resistance, followed by the black and transparent COP specimens. White samples, both PC and PC copolymer, show significantly higher mar resistance. At this moment, the only explanation for such a phenomenon is the different color, since the surface roughness values was comparable for all the tested samples (Figure 14a). The color of the undamaged area is therefore responsible for the improved mar resistance, as it was previously demonstrated for scratch resistance. Since the damaged area undergoes a whitening/brightening phenomenon, the contrast is reduced for the same reasons that have been explained so far. Five people were also asked to rank the materials according to the severity of the damage thereon. They all agreed that there was no substantial difference between the black and transparent samples. They also stated that white samples instead showed higher mar resistance and no relevant difference between PC and COP was observed. This agrees well with what was found and validate the proposed methodology, based on the experimental procedure and image analysis presented.

To sum up, the present work shows that the scratch and mar visibility depends on the surface color. This relationship holds true for both glossy and matte surfaces; therefore, the color of the samples seems to have a fundamental role in delaying the onset of visibility. This is a starting point for further study related to such phenomenon. However, significant work has yet to be done to understand how these factors play a role in the visibility. It would be useful to widen the array of tested samples for both glossy and matte surfaces. As mentioned, it is necessary to develop a physical model able to describe the interaction between light and scratch/mar, as a function of the illumination angle and observer position, predicting brightening or shadowing effect and trying to understand why, in our case, the worst-case scenario is happening at  $30^\circ$ . Also, the understanding of how these phenomena relate to the human eye perception is fundamental to develop proper descriptive quantitative models.

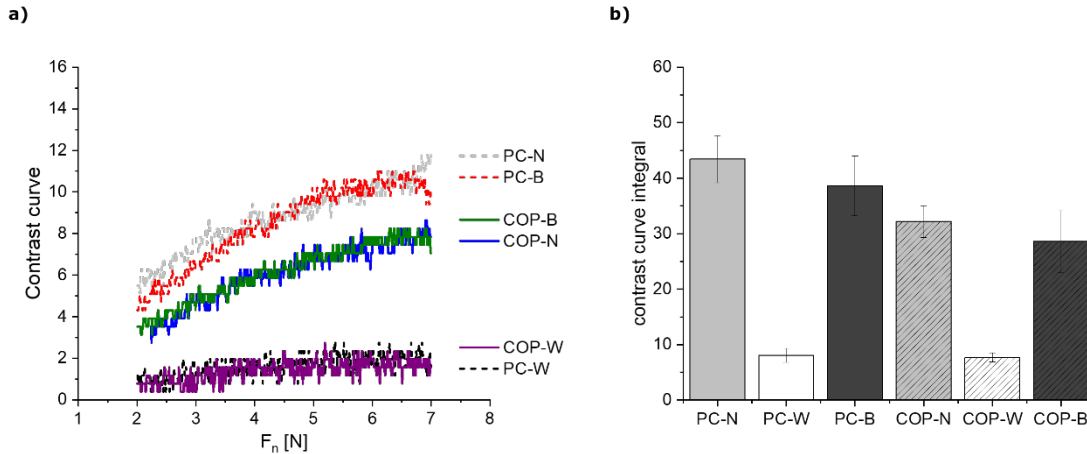


Figure 15. The image analysis gives the contrast curve reported on the left; the area under each curve was estimated and reported in the graph of the right.

#### 4. Conclusions

Scratch and mar visibility assessment on a set of model polycarbonate samples with different surface finish and color were studied by defining a standardized procedure. The results were compared and showed good agreement with human eye perception assessment, indicating how the contrast setting can be taken as a representative parameter to match human perception. It was shown that the white color delays the onset of visibility, and the reason for such phenomenon lies in the contrast difference reduction between damaged and undamaged surfaces, with damaged ones typically showing the appearance of white features. It is worth noticing that the onset of visibility is not varying with the selected contrast value for black and transparent samples. This explains why black and transparent samples show lower scratch visibility resistance compared to white samples. On the other hand, the white color masks the onset of visibility, a fact that agrees with the results of human eye assessment. The white color also decreases mar visibility because of a reduction in the contrast between the marred region and the undamaged surface. These results demonstrate how the present approach can describe and quantify the color dependence of scratch visibility, regardless of the involved deformation mechanism (ductile ploughing or marring). These findings represent an optimal starting point for further studies of the scratch and mar visibility resistance as a function of color.

#### Acknowledgments

The authors would like to acknowledge the support of SABIC's specialties business, the Texas A&M Scratch Behavior Consortium and BM Plastic (Italy).

SABIC and brands marked with <sup>TM</sup> are trademarks of SABIC or its subsidiaries or affiliates, unless otherwise noted.

© 2022 Saudi Basic Industries Corporation (SABIC). All Rights Reserved.

Any brands, products or services of other companies referenced in this document are the trademarks, service marks and/or trade names of their respective holders.

## References

- [1] C. Xiang, H.J. Sue, J. Chu, B. Coleman, *Journal of Polymer Science Part B: Polymer Physics* 39 (2001) 47-59.
- [2] V. Jardret, P. Morel, *Progress in organic coatings* 48 (2003) 322-331.
- [3] Y. Hara, T. Mori, T. Fujitani, *Progress in organic coatings* 40 (2000) 39-47.
- [4] H. Pelletier, C. Mendibide, A. Riche, *Progress in Organic Coatings* 62 (2008) 162-178.
- [5] P. Kurkcu, L. Andena, A. Pavan, *Wear* 290 (2012) 86-93.
- [6] C. Gauthier, R. Schirrer, *Journal of Materials Science* 35 (2000) 2121-2130.
- [7] L. Andena, S. Tagliabue, A. Pavan, A. Marengi, M. Testa, R. Frassine, *Polymer Testing* 89 (2020) 106602.
- [8] D. Saviello, L. Andena, D. Gastaldi, L. Toniolo, S. Goidanich, *Journal of Applied Polymer Science* 135 (2018) 46194.
- [9] H. Jiang, R. Browning, H.-J. Sue, *polymer* 50 (2009) 4056-4065.
- [10] B.J. Briscoe, P.D. Evans, E. Pellilo, S.K. Sinha, *Wear* 200 (1996) 137-147.
- [11] B.J. Briscoe, E. Pelillo, S.K. Sinha, *Polymer Engineering & Science* 36 (1996) 2996-3005.
- [12] J.-L. Bucaille, C. Gauthier, E. Felder, R. Schirrer, *Wear* 260 (2006) 803-814.
- [13] M.M. Hossain, H. Jiang, H.-J. Sue, *Wear* 270 (2011) 751-759.
- [14] J. Bucaille, E. Felder, G. Hochstetter, *Wear* 249 (2001) 422-432.
- [15] H. Jiang, G. Lim, J. Reddy, J. Whitcomb, H.J. Sue, *Journal of Polymer Science Part B: Polymer Physics* 45 (2007) 1435-1447.
- [16] L. Van Breemen, L. Govaert, H. Meijer, *Wear* 274 (2012) 238-247.
- [17] R. Hadal, R. Misra, *Materials Science and Engineering: A* 398 (2005) 252-261.
- [18] H. Jiang, R.L. Browning, M.M. Hossain, H.-J. Sue, M. Fujiwara, *Applied Surface Science* 256 (2010) 6324-6329.
- [19] L.-P. Sung, P.L. Drzal, M.R. Vanlandingham, A.M. Forster, *Metrology for characterizing the scratch resistance of polymeric coatings through optical scattering*, Tribology and Interface Engineering Series, vol 51, Elsevier, 2006, pp. 102-123.
- [20] P. Rangarajan, M. Sinha, V. Watkins, K. Harding, J. Sparks, *Polymer Engineering & Science* 43 (2003) 749-758.
- [21] J.-I. Weon, S.-Y. Song, K.-Y. Choi, S.-G. Lee, J. Lee, *Journal of materials science* 45 (2010) 2649-2654.
- [22] J.-I. Weon, I.-H. Cho, S.-Y. Song, J.-B. Lee, K.-Y. Choi, S.-G. Lee, J.H. Lee, *Macromolecular Research* 18 (2010) 610-613.
- [23] M. Hamdi, H.-J. Sue, *Materials & design* 83 (2015) 528-535.
- [24] M. Hamdi, D. Manica, H.-J. Sue, *SAE International Journal of Materials and Manufacturing* 10 (2017) 94-106.
- [25] J. Chrisman, S. Xiao, M. Hamdi, H. Pham, M.J. Mullins, H.-J. Sue, *Polymer Testing* 69 (2018) 238-244.
- [26] I. Hutchings, P. Wang, G. Parry, *Surface and Coatings Technology* 165 (2003) 186-193.
- [27] C. Barr, L. Wang, J. Coffey, F. Daver, *Journal of materials science* 52 (2017) 1221-1234.
- [28] P. Gamonal-Repiso, M. Sánchez-Soto, S. Santos-Pinto, M.L. Maspocho, *Wear* 440 (2019) 203082.
- [29] K. Noh, J. Fincher, R. Mimms, H.-J. Sue, *Polymer* 223 (2021) 123709.
- [30] B. Wang, K.J. Ciuffreda, *Surv Ophthalmol* 51 (2006) 75-85.
- [31] A.A. Michelson, *Studies in optics*, Courier Corporation, 1995.
- [32] E. Peli, *JOSA A* 7 (1990) 2032-2040.
- [33] K.J. Kim, R. Mantiuk, K.H. Lee, *Measurements of achromatic and chromatic contrast sensitivity functions for an extended range of adaptation luminance*, Human vision and electronic imaging XVIII, vol 8651, SPIE, 2013, pp. 319-332.
- [34] T.D. Lamb, *Eye* 30 (2016) 179-185.
- [35] R. Hess, E. Howell, *Vision research* 17 (1977) 1049-1055.

- [36] E.C. Amesbury, S.C. Schallhorn, *International ophthalmology clinics* 43 (2003) 31-42.
- [37] S. Drew, Draft Report, Griffith University, Australia (2005).
- [38] P.G. Barten, Formula for the contrast sensitivity of the human eye, *Image Quality and System Performance*, vol 5294, SPIE, 2003, pp. 231-238.
- [39] P.G. Barten, Contrast sensitivity of the human eye and its effects on image quality, SPIE press, 1999.
- [40] BS EN ISO 2813:2014, Paints and varnishes - Determination of gloss value at 20 degrees, 60 degrees and 85 degrees., 2014.
- [41] H. Jiang, R. Browning, J. Fincher, A. Gasbarro, S. Jones, H.-J. Sue, *Applied Surface Science* 254 (2008) 4494-4499.
- [42] E. Amerio, P. Fabbri, G. Malucelli, M. Messori, M. Sangermano, R. Taurino, *Progress in Organic Coatings* 62 (2008) 129-133.
- [43] S.A. Shafer, *Color Research & Application* 10 (1985) 210-218.
- [44] I.D. Nikolov, C.D. Ivanov, *Applied Optics* 39 (2000) 2067-2070.
- [45] N.G. Sultanova, I.D. Nikolov, C.D. Ivanov, *Optical and quantum electronics* 35 (2003) 21-34.
- [46] R. Browning, M.M. Hossain, J. Li, S. Jones, H.-J. Sue, *Tribology international* 44 (2011) 1024-1031.